Estimation of Design Parameters for Braced Excavation: Numerical Study

Subha Sankar Chowdhury[1]; Kousik Deb[2]; and Aniruddha Sengupta[3]

Abstract: This paper discusses the development of a numerical model for a braced excavation to estimate the various design parameters that significantly influence the excavation's behavior. The results of the numerical model were compared with those of a reported case study of a braced excavation in sand, and close agreement between the results was observed. The developed model is used for parametric study to show the influence of different design parameters, such as strut stiffness, wall thickness, strut arrangement and the embedded depth of the wall on strut force, maximum moment developed in the wall, maximum lateral displacement of the wall, and maximum vertical displacement of ground surface. It was found that, among all the combinations studied, a particular type of strut arrangement for a particular ratio of embedded depth and excavation depth produces the best possible result. A design guideline is also presented based on the results of this numerical study. **DOI: 10.1061/(ASCE)GM.1943-5622.0000207.**

CE Database subject headings: Bracing; Excavation; Displacement; Parameters; Struts; Walls; Bending; Numerical analysis.

Author keywords: Braced excavation; FLAC; Stiffness; Displacement; Embedded depth; Design parameters; Strut force; Wall thickness; Wall bending moment.

Introduction

Deep underground excavation is extremely important in the construction of underground transport systems, basements, water pipelines, and other structures that are to be located at a substantial depth below the ground surface. In underground excavation, sufficient space is not available for stability of the excavated slope because this type of excavation is done in congested urban areas. Thus, this type of excavation is made vertically, below the ground surface, and the excavated soil surface is retained with the help of a wall, which may be in the form of a sheet pile, a diaphragm, or soldier piles, with timber lagging so that soil does not fall within the construction zone. In urban areas, many buildings and roads are located near construction areas. As the excavation progresses, the retaining wall is supported by horizontal members known as struts. Lateral displacement of the wall and vertical displacement of the ground surface occur simultaneously, which may, in turn, directly affect the stability of the surrounding infrastructures. Thus, one of the critical aspects of underground excavation is the settlement of the adjacent ground. Boscardin and Cording (1989) found that the profiles of settlements and horizontal strain induced in the structure are vital because they determine the level of damage in the structure. Thus, it is extremely important to evaluate the vertical deformations of the ground surface so that remedial measures can be taken to minimize them. The lateral displacement of the wall is also important, because if this deformation is not within the acceptable limit, it may cause the entire underground support system to fail. The bending moments developed in the wall and strut forces are also very important factors that must be evaluated when designing braced excavation systems.

Most studies on deep excavation have been based on analytical and numerical modeling. The FEM has been used to study earth pressures, strut loads, bending moments, and horizontal deflection for a strutted sheet pile and ground settlement pattern (Ng and Lings 1995; Vaziri 1996; Ng. et al. 1998; Karlsrud and Andresen 2005; Zdravkovic et al. 2005; Costa et al. 2007; Kung et al. 2009; Kung 2009; Chungsik and Dongyeob 2008). With the help of the FEM, a parametric study of a 13.6-m-deep braced excavation was carried out by Bose and Som (1998), who found that the width of the excavation influences the soil-wall deformations and that prestressing the struts has a marked effect on the performance of such a braced cut. Finno et al. (2007) observed that when the ratio of excavated length to excavated depth of a wall is greater than 6, plane strain simulations yield the same displacements in the center of that wall as those of a three-dimensional simulation. Hsiung (2009) studied the effect of soil elasticity, creep, and soil–wall interface by numerical analysis and compared the results of the numerical model with a case study of excavation in sand. de Lyra Nogueira et al. (2009) conducted a finite-element analysis on excavations in saturated soil by using coupled deformation and flow formulation for different constitutive models and different excavation rates. It was observed that the constitutive models affected the magnitude and distribution of excess pore water pressures. In addition, it was concluded that excavation rates that are one order of magnitude lower than the hydraulic conductivity of the soil represent drained processes in efficiently. Babu et al. (2011) used the finite difference tool Fast Lagrangian Analysis of Continua (FLAC) (Itasca) to perform a two-dimensional (2D) numerical analysis of a vibration-isolated system using open trenches. The numerical model was first calibrated with respect to material properties, damping value, and

[1]Research Scholar, Dept. of Civil Engineering, Indian Institute of Technology Kharagpur, Kharagpur 721302, India. E-mail: chowdhurysubha@gmail.com

[2]Assistant Professor, Dept. of Civil Engineering, Indian Institute of Technology Kharagpur, Kharagpur 721302, India (corresponding author). E-mail: kousik@civil.iitkgp.ernet.in

[3]Associate Professor, Dept. of Civil Engineering, Indian Institute of Technology Kharagpur, Kharagpur 721302, India. E-mail: sengupta@civil.iitkgp.ernet.in

Note. This manuscript was submitted on August 2, 2011; approved on January 12, 2012; published online on January 14, 2012. Discussion period open until November 1, 2013; separate discussions must be submitted for individual papers. This paper is part of the ***International Journal of Geomechanics***, Vol. 13, No. 3, June 1, 2013. ©ASCE, ISSN 1532-3641/2013/3-234–247/$25.00.

Int. J. Geomech. 2013.13:234-247.

boundary conditions, and the output was compared with results obtained from field vibration tests at a proposed site. After comparing the results of the parametric study (accomplished by varying input motion, depth of cutoff trench, etc.) with the human level of perception, a decision regarding the vibration isolation system was made. With the help of the Nonlinear Analysis of Geotechnical Problems (ANLOG) code, Nogueira et al. (2011) presented the finite-element simulation of an instrumented, unsupported excavation made in a soft clay deposit using a nonassociated elastoplastic constitutive model. Close agreement between the in-situ monitored results of both displacement and pore water pressures and the results obtained from a numerical simulation was observed. Numerical modeling is also used broadly to predict ground deformation caused by excavation (Finno and Harahap 1991; Hsi and Small 1993; Whittle et al. 1993; Hashash and Whittle 2002). In addition to numerical modeling, empirical and semiempirical methods are often used for estimating the ground surface settlement induced by an excavation (Bowles 1988; Ou et al. 1993; Hsieh and Ou 1998).

Tefera et al. (2006) studied the ground settlement and wall deformation of a sheet pile wall during different stages of an excavation using a large-scale model test with dry sand and compared the results with finite-element simulations. Nakai et al. (1999) performed 2D model tests with aluminum rods in place of sand and analyzed them with an elastoplastic FEM. It was found that the computed results closely matched the results obtained from the model tests. Seok et al. (2001) performed model tests to quantify the amount of building settlement adjacent to a braced excavation and the zone of soil improvement required to reduce building settlement when the building's centroid is located within the excavation influence zone.

A number of factors, such as the number of props, their stiffness and vertical spacing, and the wall stiffness and its embedded depth and thickness, are involved in the stability of a braced excavation system and the adjacent ground. In the current study, numerical analysis was conducted to show the influence of these factors on the behavior of the wall and the adjacent ground, and a range of values for the parameters (i.e., the number of struts, their positions and stiffness, the thickness of the wall and its embedded depth) is suggested so that an optimum result can be achieved in terms of axial force or strut force, bending moment, lateral displacement of the wall, and vertical displacement of the ground surface.

Numerical Modeling

The numerical analysis was carried out as a plane strain problem using the computer program FLAC. The definitions of the symbols used in the analysis are shown in Fig. 1. In Fig. 1, D_e is the maximum excavation depth (final stage), D_b is the embedded depth (final stage), h_i is the vertical spacing of supports (struts), t_{wall} is the thickness of the wall, u is the maximum horizontal wall displacement, ν is the maximum vertical ground displacement, and N is the number of support layers. The soil is assumed to be dry above the water table and fully saturated below it. The analysis was carried out under undrained conditions, and the excavation process was simulated according to the following sequence:

1. Wall installation: A wished-in-place wall is adopted and installation effects are ignored,
2. Dewatering: Dewatering is carried out within the excavated zone up to the desired excavated level before the actual excavation is simulated,
3. Excavation: The excavation is carried out up to a certain depth below the corresponding strut level, and
4. Installation of strut: After the excavation is carried, the strut is installed at the desired depth below the ground surface.

This construction sequence (Step 2 to Step 4) was followed for each level until the final excavation level was reached. The numerical analysis was conducted and validated using a case study presented by Hsiung (2009). For validation of the numerical model, site conditions and the geometry of the excavation as reported for the case study (Hsiung 2009) were used. The excavation was 194 m long and 20.7 m wide. The excavation was carried out up to a depth of 19.6 m. The wall of the excavation was supported by a 1-m-thick, 36-m-deep concrete diaphragm wall. The Young's modulus (E_{wall}), cross-sectional area (A_{wall}), and moment of inertia (I_{wall}) were specified for the diaphragm wall. Considering unit length along the length of the wall, A_{wall} was calculated as thickness $(t_{wall}) \times 1.0$ (i.e., t_{wall}). The wall was supported by steel struts at various levels. The struts were spaced horizontally at a distance of 4.5 m center to center along the length of the excavation. For the struts, horizontal spacing (s), cross-sectional area (A_{strut}), Young's modulus (E_{strut}), moment of inertia (I_{strut}), and density of strut material were specified. Descriptions of the struts are given in Table 1. A typical cross section of the excavation used in the validation study is shown in Fig. 2. The soil profile consisted of 60 m of silty fine sand with occasional bands of silty clay. A description of the ground profile and related soil parameters is given in Table 2. The cohesion of the sand and bands of silty clay was assumed to be zero as adopted by Hsiung (2009).

The mesh and the boundary condition of the validation model are shown in Fig. 3. The horizontal boundary of the analytical mesh was set at 60 m below ground level (GL). A 2D plane strain analysis was performed, and the center of the excavation was set at one vertical boundary. The other vertical boundary was set at 200 m from the wall. Both horizontal and vertical movements were restrained along the bottom boundary, and the vertical boundaries were restrained only against horizontal movements. In the model, the water level was set at 3 m below the ground surface.

An elastic-perfect plastic "Mohr-Coulomb" model was used to model the soil. The soil unit weight (γ) and the effective friction angle (ϕ') as reported by Hsiung (2009) were used in the current

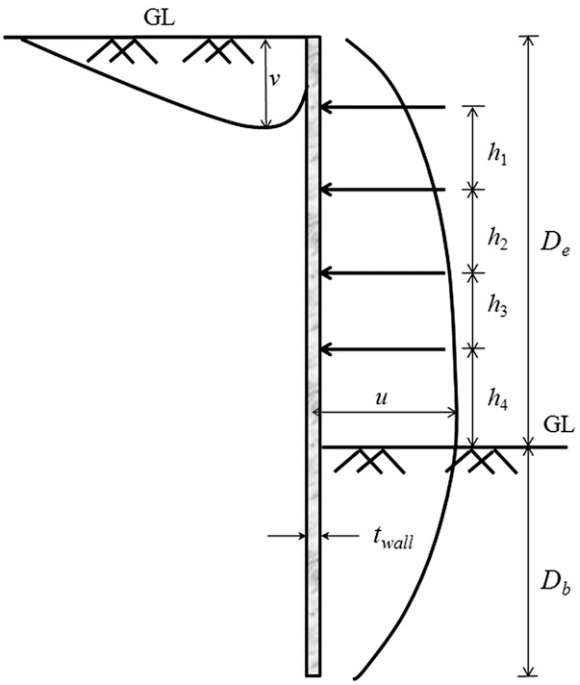

Fig. 1. Symbols used in the analysis

Int. J. Geomech. 2013.13:234-247.

Table 1. Description of Struts Used in Validation Study

Strut number	Depth of strut below ground surface (m)	Sections provided	Density (kg/m^3)	Cross-sectional area (m^2 × 10^{-4})	Moment of inertia (m^4 × 10^{-8})
1	2.5	H350 × 350 × 12 × 19	7,850.0	173.9	40,800
2	5.9	H400 × 400 × 13 × 21	7,850.0	218.7	66,600
3	9.1	2H414 × 405 × 18 × 28	7,850.0	590.8	185,600
4	12.6	2H414 × 405 × 18 × 28	7,850.0	590.8	185,600
5	15.8	2H414 × 405 × 18 × 28	7,850.0	590.8	185,600

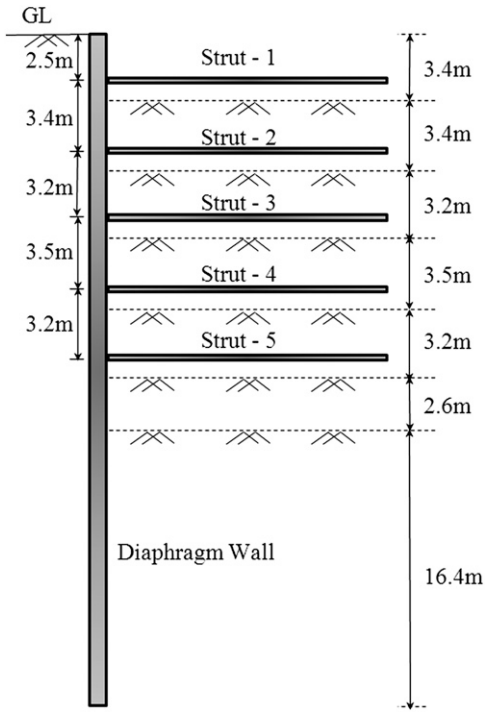

Fig. 2. Cross section of the excavation for validation study (data from Hsiung 2009)

model. In the analysis, the effective cohesion (c') for the soil was set at zero. The coefficient of lateral earth pressure at rest (K_o) was taken from Jaky's equation (i.e., $1-\sin\phi'$). Here, K_o was set at 0.455, based on ϕ' equal to 33°. The stiffness, E, for each of the soil layers was calculated based on the relationship given by Hsiung (2009) as $E = 2000N$ (in kPa), where N is the average Standard Penetration Test value (SPT-N) of each soil layer as obtained from the site. Bulk modulus (K) and shear modulus (G) were calculated as

$$K = \frac{E}{3(1-2\mu)} \tag{1}$$

$$G = \frac{E}{2(1+\mu)} \tag{2}$$

where μ = Poisson's ratio of soil. In the current study, μ for the soil was set at 0.30.

The interface parameters, including the friction angle and the normal and shear stiffness (K_n and K_s), were estimated from the soil parameters (i.e., drained friction angle, bulk modulus, and shear modulus). The interface normal and shear stiffness were selected such that the stiffness was approximately 10 times the equivalent stiffness of the stiffest neighboring zone as suggested by the FLAC manual (Itasca 2005). The value of the equivalent stiffness of a zone normal to the interface is given by

$$\frac{\left(K+\frac{4}{3}G\right)}{\Delta z_{\min}} \tag{3}$$

where $\Delta z_{\min}$ = smallest width of adjoining zone in normal direction to the interface. In the validation model, the equivalent stiffness was calculated as 9.1×10^7 N/m^2. Thus, the values of the interface normal and shear stiffness (i.e., K_n and K_s) were set at 9.1×10^8 N/m^2. The interface friction angle was set at two-thirds of the maximum soil friction angle.

The values of E_{wall} and Poisson's ratio (μ_{wall}) of the diaphragm wall are not mentioned in Hsiung (2009). Therefore, the values of these two parameters were taken from Bose and Som (1998) as 2.5×10^7 kN/m^2 and 0.15, respectively, for the concrete diaphragm wall. The wall was modeled by beam elements, with the value of Young's modulus as $E_{\text{wall}}/(1-\mu_{\text{wall}}{}^2)$ to represent the plane stress formulation for the structural elements in the plane-strain condition of a continuous wall as noted in the FLAC manual. The struts were steel members and were also modeled as beam elements, with $E_{\text{strut}} = 2 \times 10^8$ kN/m^2. The boundary conditions at the ends of the struts were modeled by springs. The spring was connected to the node at the proposed strut level. The strut was also connected to the other node, which was on the line of symmetry (i.e., at the centerline of the excavation), with the help of a similar spring. The connection between the strut and the wall was pin jointed (i.e., no resistance to rotation was provided).

Results and Discussion

Validation

To validate the developed numerical model, the results of the model were compared with the predicted values (based on numerical study) and observed values (based on field study) as reported by Hsiung (2009). In the numerical analysis, Hsiung (2009) used an elastic-perfect plastic "Mohr-Coulomb" model for the soil. In this analysis, Hsiung (2009) used soil stiffness calculated from shear wave velocity and SPT-N and reduced SPT-N values. However, in the current study, the numerical results based on SPT-N values obtained by Hsiung (2009) were used for the comparison. Fig. 4 shows the ground surface settlement at an excavation depth of 19.6 m below the ground surface. The variations in lateral displacement of the wall with excavation depths of up to 3.4 m and 19.6 m are shown in Figs. 5(a and b), respectively. It can be seen in Fig. 4 that within a distance of 50 m from the edge of the excavation, the settlement values predicted by the present model match the observed values more closely than do those predicted by Hsiung (2009). The current model predicted larger ground settlements than those predicted by Hsiung (2009), but as

Int. J. Geomech. 2013.13:234-247.

Table 2. Description of Ground Profile and Related Soil Parameters (Data from Hsiung 2009)

Depth below ground level (m)	Description of soil	Approximate total unit weight (kN/m^3)	c' (kN/m^2)	ϕ' (degree)	SPT-N value	Water content (%)
0.0–7.5	Yellow and gray silty sand	19.7	0	32	5–14	4.9–22.3
7.5–10.0	Gray silty clay with sandy silt	18.6	0	30	4	29.6–41.4
10.0–22.5	Gray silty sand, occasionally with sandy silt	19.6	0	32	6–22	22.9–32.5
22.5–25.0	Gray silty clay with silt	19.3	0	33	12–16	20.3
25.0–29.5	Gray silty sand with sandy silt	19.7	0	33	19–29	26.6–30.6
29.5–32.0	Gray silty clay	19.5	0	32	13–19	28.2
32.0–60.0	Gray silty sand with clay	19.9	0	33	28–42	22.4–32.2

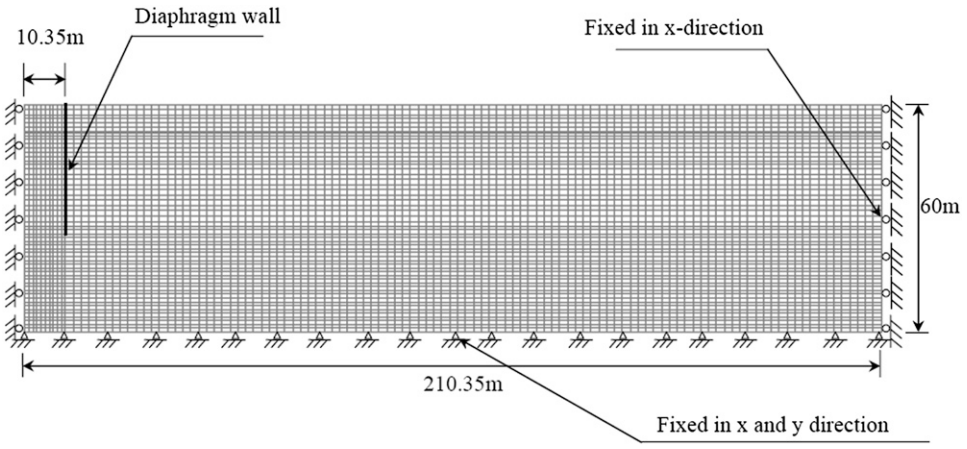

Fig. 3. Mesh used in the validation study

the distance from the edge of the excavation increases, the differences between the two results gradually diminish.

In Fig. 5(a), it can be seen that for excavations up to 3.4 m in depth, the lateral displacement obtained from the current model more closely matches the results predicted by Hsiung (2009) as compared with the observed settlements. However, for a 19.6-m excavation depth, the results obtained from the current study more closely match the observed values, as compared with the results predicted by Hsiung (2009) [as shown in Fig. 5(b)]. In Fig. 5(a), it can be seen that the lateral displacement of the wall predicted by the current analysis is greater than that predicted by Hsiung (2009) when the depth of the wall is greater than 10 m, but that this is the opposite near the ground surface. When the excavation depth is up to 19.6 m, the lateral wall displacement is greater than that predicted by Hsiung (2009) when the depth of the wall is greater than 5 m. As shown in Figs. 5(a and b), the predicted lateral displacement values at the two excavation depths are always greater than the observed values.

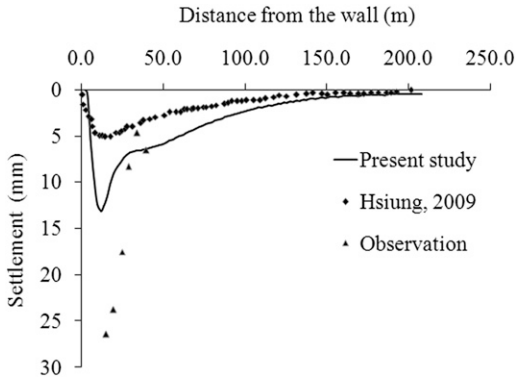

Fig. 4. Observed and predicted ground surface settlement at 19.6-m excavation depth

Parametric Study

After the numerical model was validated, a parametric study was carried out for two different soil profiles, each consisting of four layers. The first profile (Profile 1) consisted of soil layers in which their stiffness increased with depth (i.e., the weakest soil was at the top and the strongest at the bottom). In the second profile (Profile 2), the weakest layer was below the first layer of soil. Below the weakest layer, the soil stiffness increased with depth. The two soil profiles are described in Table 3. The Young's modulus (E) was obtained from the correlation given by Papadopoulus (Som and Das 2006) as $E = 75 + 8N$ kg/cm^2 (1 kg/cm^2 = 100 kN/m^2), where N is the SPT blow count. The width of the excavation, B, was set at 20 m and was kept constant for all the parametric studies. Excavation depths of 10 m, 15 m, and 20 m were considered. With various excavation depths, the position of the struts, the embedded depth of the wall, the stiffness of the struts, and the thickness of the wall were varied to study their influence on major design factors, such as (1) maximum strut force at each level, (2) maximum bending moment in the wall, (3) maximum lateral displacement of the wall, and (4) maximum ground surface displacement. The position and number of struts were varied for different embedded depths to study their effect on the aforementioned factors. The different arrangements of struts that were studied (i.e., types A, B, and C) are presented in Table 4.

When the depth of the excavation (D_e) was equal to 20 m, four levels of struts were considered at different positions and the analysis was carried out with $t_{wall} = 0.8$ m, with varying embedded depth

Int. J. Geomech. 2013.13:234-247.

ratios D_b/D_e from 0.4 to 1.4 and keeping the strut stiffness at $k_{strut} = 5.0 \times 10^5$ kN/m/m to show the effect of the position of the struts. Among all the combinations with four levels of struts, only System 3A (first-, second-, third-, and fourth-level struts placed at 2 m, 7 m, 12 m, and 17 m below GL, respectively) was studied by varying the wall thickness from 0.8 m to 1.6 m and the strut stiffness from 1×10^5 kN/m/m to 125×10^5 kN/m/m to show the effect of wall thickness and strut stiffness. When the depth of the excavation was 10 m (Systems 1B to 5B), two levels of struts were considered at different positions, and the analysis was conducted with $t_{wall} = 0.80$ m, $D_b/D_e = 1.0$, and $k_{strut} = 5 \times 10^5$ kN/m/m. Among all the combinations with two levels of struts, only System 1B (first- and second-level struts placed at 2 m and 6 m below GL, respectively) was analyzed by varying strut stiffness, k_{strut}, from 1×10^5 kN/m/m to 125×10^5 kN/m/m. Similarly, when the depth of the excavation was 15 m (Systems 1C to 5C), three levels of struts were considered at different positions and the analysis was carried out with $t_{wall} = 0.80$ m, $D_b/D_e = 1.0$, and $k_{strut} = 5 \times 10^5$ kN/m/m Only System 2C (first-, second-, and third-level struts placed at 2 m, 6 m, and 11 m below GL, respectively) was analyzed by varying the strut stiffness, k_{strut}, from 1×10^5 kN/m/m to 125×10^5 kN/m/m to show the effect of strut stiffness.

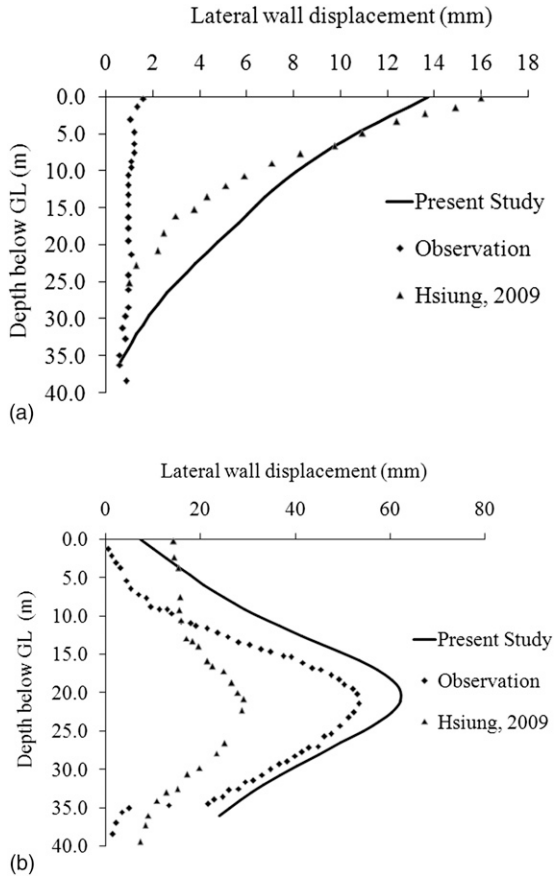

Fig. 5. Comparison of observed and predicted lateral displacement of wall: (a) 3.4-m excavation depth; (b) 19.6-m excavation depth

Effect of Embedded Depth

The embedded depth (D_b) was normalized with respect to the maximum excavation depth (D_e), and the effect of the nondimensional parameter D_b/D_e on the maximum strut force at each level, maximum bending moment in the wall, maximum lateral deflection of the wall, and maximum ground surface settlements were studied. The maximum force in each strut is shown in Table 5 and the maximum moment (M) in the wall is shown in Figs. 6(a and b) for different strut arrangements (for System 1A to System 6A). As Table 5 shows, for most of the cases of a particular strut arrangement, the value of the maximum strut force first decreased with increasing D_b/D_e and then attained a minimum value for D_b/D_e equal to 0.8–1.0; after that, it either remained constant or increased slightly. However, the change in maximum strut force value with the change in D_b/D_e was marginal (except at the fourth level of struts). The maximum variations (between the highest and lowest strut force under different D_b/D_e values) of strut forces in the first, second, third, and fourth level for Profiles 1 and 2 were 5%, 1.6%, 3.75%, and 15%, and 1.1%, 3.1%, 6%, and 13.6%, respectively, for System 3A. Similarly, from Figs. 6(a and b) it can be seen that in most cases, the maximum wall moment attained a minimum value when D_b/D_e was 0.80–1.0, after which there was no substantial change in values. This happened because the passive resistance below the base of the excavation increased up to a certain limit, after which it remained constant with the increase of embedded depth below the final excavation level. It was observed that in System 3A, under different D_b/D_e values, the maximum variations in maximum wall moment were 5.17% and 6.87% for Profiles 1 and 2, respectively.

The maximum horizontal wall displacement and maximum vertical ground displacement were calculated for different strut arrangements (Systems 1A to 6A). The variations in maximum horizontal wall displacement and maximum vertical ground displacement with D_b/D_e are shown in Figs. 7(a and b) and 8(a and b), respectively, for two different soil profiles. As seen in Figs. 7(a and b), in most of the strut arrangements, the maximum lateral wall displacement decreased initially with increasing D_b/D_e (except for System 2A) and then attained a minimum value for D_b/D_e equal to 0.8–1.0, after which it remained constant for both the profiles. In Figs. 7(a and b), it can be seen that in System 3A, the maximum variations in maximum lateral wall displacement were 5.25% and 5.3% for Profiles 1 and 2, respectively. Similarly, in Figs. 8(a and b), it can be seen that in System 3A, the maximum variations in the

Table 3. Description of Soil Profiles Considered in Parametric Study

Soil profile type	Depth below ground level (m)	Layer number	SPT-N value	Total unit weight (kN/m^3)	c' (kN/m^2)	ϕ' (degree)	Poisson's ratio, μ	E (kN/m^2)
Profile 1	0.0–5.0	1	5	18.8	0	30	0.3	11,500
	5.0–15.0	2	10	19.0	0	32	0.3	15,500
	15.0–30.0	3	15	19.5	0	33	0.3	19,500
	30.0–60.0	4	30	19.8	0	34	0.3	31,500
Profile 2	0.0–5.0	1	5	18.8	0	30	0.3	11,500
	5.0–15.0	2	2	17.5	0	20	0.3	9,100
	15.0–30.0	3	15	19.5	0	33	0.3	19,500
	30.0–60.0	4	30	19.8	0	34	0.3	31,500

Int. J. Geomech. 2013.13:234-247.

values of maximum vertical ground displacement were 51% and 27.1% for Profiles 1 and 2, respectively. Thus, it appears that a change in D_b/D_e value significantly affected the maximum vertical ground displacement, as compared with the other design factors. It is further observed from the plots that in most cases, the range of values of maximum axial force, maximum wall moment, maximum lateral wall displacement, and maximum vertical ground displacement were lowest if the D_b/D_e value was kept within the range of 0.8 to 1.0. However, the most sensitive design factor was maximum vertical ground displacement with respect to D_b/D_e value. Thus, if the embedded depth was kept between 80% and 100% of the excavation depth, then the moments and displacements (both lateral and vertical) would be as low as possible and the strut force would also be in the lower range.

Table 4. Different Types of Arrangements of Struts Used in Parametric Study

Arrangement type	System number	D_e (m)	Depth of each strut below ground level (m)			
			1st strut	2nd strut	3rd strut	4th strut
A	1A	20.0	2	6	11	16
	2A		2	6	10	15
	3A		2	7	12	17
	4A		3	7	11	16
	5A		3	7	11	17
	6A		3	8	13	18
B	1B	10.0	2	6	—	—
	2B		2	7	—	—
	3B		3	6	—	—
	4B		3	7	—	—
	5B		3	8	—	—
C	1C	15.0	2	6	10	—
	2C		2	6	11	—
	3C		2	7	12	—
	4C		3	7	11	—
	5C		3	8	13	—

Effect of Position of Struts

The effects of different strut arrangements on the maximum strut force at each level, maximum bending moment in the wall, maximum lateral deflection of the wall, and maximum ground surface settlements were studied for different ratios of D_b/D_e. The location of each strut below GL (i.e. their position below GL) was normalized with D_e.

It can be seen from Table 5 that the force in a particular strut depended primarily on the position of that strut in the system. It can also be seen that the maximum force in a strut at a particular level depended on the vertical distance between two consecutive struts. As the vertical distance between two consecutive struts increased, the force in the top strut also increased. This is because a strut experiences maximum force when the excavation is done, before installation of the next strut. Thus, the greater the difference in height between the two struts, the greater the force in the top strut. In Table 5 it can be seen that for a ratio of D_b/D_e equal to 0.80, the forces in the first-, second-, third-, and fourth-level struts were lowest in Systems 3A, 2A, 2A, and 6A, respectively, when Profile 1 was considered. For Profile 2, the forces in the first-, second-, third-, and fourth-level struts were lowest in Systems 4A, 2A, 2A, and 6A, respectively. At $D_b/D_e = 0.8$, the maximum variations (between the highest and lowest strut force under different strut arrangements) of strut force at the first, second, third, and fourth levels were 26.5, 88, 31, and

Table 5. Variations in F with D_b/D_e for System 1A to 6A for Profiles 1 and 2

System number	Strut number	Depth of strut/D_e	$F \times 10^3$ (kN/m)											
			$D_b/D_e = 0.4$		$D_b/D_e = 0.6$		$D_b/D_e = 0.8$		$D_b/D_e = 1.0$		$D_b/D_e = 1.2$		$D_b/D_e = 1.4$	
			Profile 1	Profile 2	Profile 1	Profile 2	Profile 1	Profile 2	Profile 1	Profile 2	Profile 1	Profile 2	Profile 1	Profile 2
1A	1	0.10	4.93	5.85	4.92	5.78	4.95	5.78	4.98	5.80	5.01	5.82	5.04	5.85
	2	0.30	2.03	1.93	1.97	1.88	1.96	1.86	1.94	1.87	1.93	1.86	1.93	1.87
	3	0.55	15.06	14.71	14.94	14.51	14.34	13.86	14.19	13.65	14.14	13.65	14.14	13.59
	4	0.80	13.39	14.07	12.44	13.25	12.28	13.02	11.85	12.52	11.75	12.37	11.78	12.38
2A	1	0.10	4.43	5.41	4.43	5.37	4.46	5.37	4.48	5.39	4.51	5.41	4.54	5.43
	2	0.30	1.53	1.49	1.48	1.46	1.47	1.46	1.44	1.46	1.44	1.46	1.43	1.45
	3	0.50	13.87	13.26	13.65	12.97	13.24	12.52	13.18	12.42	13.16	12.40	13.19	12.40
	4	0.75	16.65	17.85	15.94	17.19	16.80	18.04	16.18	17.38	16.19	17.20	16.15	17.26
3A	1	0.10	3.60	4.71	3.59	4.69	3.64	4.71	3.69	4.70	3.74	4.72	3.78	4.74
	2	0.35	11.20	10.89	11.11	10.67	11.02	10.55	11.02	10.55	11.05	10.55	11.08	10.56
	3	0.60	16.26	17.20	16.26	16.99	15.88	16.47	15.65	16.18	15.70	16.17	15.72	16.20
	4	0.85	8.50	8.71	7.55	7.97	7.45	7.90	7.32	7.69	7.22	7.57	7.26	7.52
4A	1	0.15	3.78	4.55	3.79	4.52	3.78	4.50	3.80	4.50	3.79	4.48	3.81	4.48
	2	0.35	9.56	10.33	9.53	10.11	9.55	10.07	9.60	10.08	9.63	10.10	9.70	10.14
	3	0.55	15.69	16.76	15.67	16.65	15.44	16.17	15.39	16.11	15.49	16.17	15.56	16.16
	4	0.80	11.92	12.53	11.10	11.75	10.87	11.61	10.83	11.49	10.88	11.63	11.05	11.83
5A	1	0.15	3.78	4.55	3.79	4.52	3.78	4.50	3.78	4.50	3.79	4.48	3.81	4.48
	2	0.35	9.56	10.32	9.53	10.09	9.54	10.07	9.61	10.08	9.63	10.10	9.69	10.14
	3	0.55	19.67	21.39	19.61	20.98	19.18	20.40	19.21	20.23	19.25	20.24	19.39	20.33
	4	0.85	8.15	8.12	7.22	7.55	7.07	7.37	7.00	7.39	7.13	7.53	7.24	7.60
6A	1	0.15	4.65	5.43	4.62	5.40	4.63	5.39	4.61	5.39	4.61	5.38	4.61	5.37
	2	0.40	12.51	12.96	12.39	12.57	12.31	12.41	12.38	12.40	12.42	12.46	12.49	12.45
	3	0.65	17.69	19.21	17.54	18.97	16.96	18.34	16.86	18.06	16.90	18.15	17.02	18.27
	4	0.90	4.28	4.33	3.68	3.83	3.77	3.83	3.72	3.96	3.82	3.97	3.96	4.04

Int. J. Geomech. 2013.13:234-247.

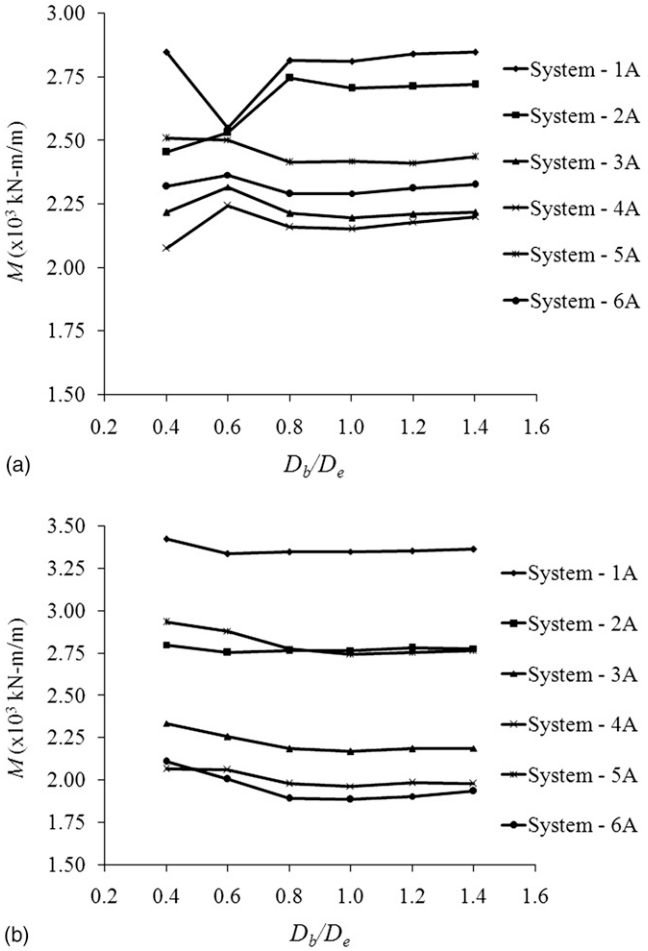

Fig. 6. Variation in M with D_b/D_e: (a) Soil Profile 1; (b) Soil Profile 2

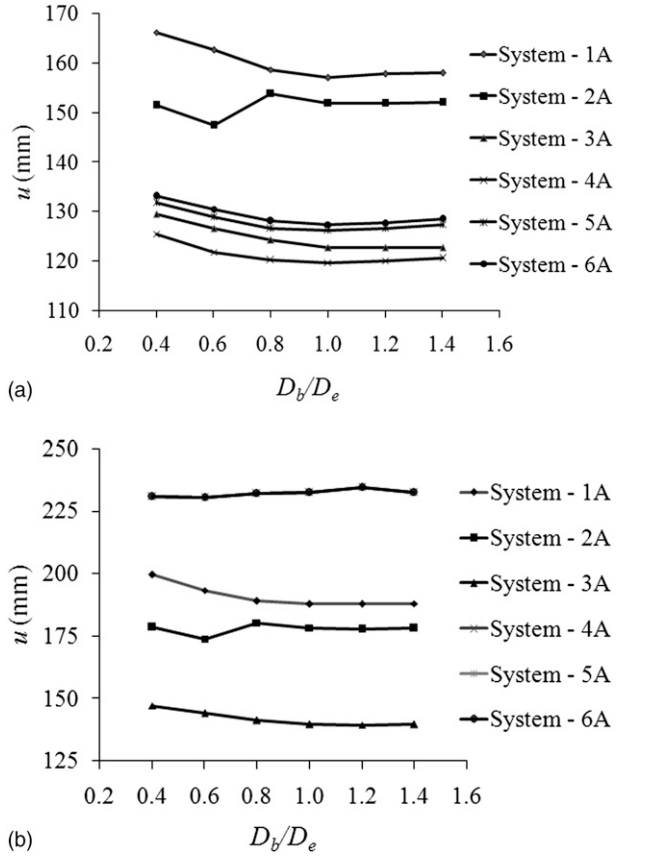

Fig. 7. Variation in u with D_b/D_e: (a) Soil Profile 1; (b) Soil Profile 2

77.6%, respectively, for Soil Profile 1. Similarly, for Soil Profile 2, the maximum variations were 22.1, 88.2, 38.6, and 78.8%, respectively.

The maximum bending moment (M) in the wall depends on the unsupported length between two support levels at any stage of excavation [as shown in Figs. 6(a and b)]. In some cases, if the initial cantilever height (i.e., after excavation and before installation of the first-level strut) is much greater, then the moment may be maximum in this stage compared with other subsequent stages. In Figs. 6(a and b), it can be seen that the lowest range of values of M was obtained for Systems 3A and 4A and Systems 4A and 6A in the case of soil Profiles 1 and 2, respectively. It was observed that at $D_b/D_e = 0.8$, the maximum variations in M were 23 and 43.6% for Profiles 1 and 2, respectively.

In Fig. 7(a), it can be seen that the lowest range of values of maximum horizontal wall movement was obtained for Systems 3A and 4A, where the first-, second-, third-, and fouth-level struts were 0.10–0.15, 0.35, 0.55–0.60, and 0.80–0.85 times the excavation depth, respectively for Profile 1. In Fig. 7(b), it can be seen that the lowest value of maximum horizontal wall movement was obtained for System 3A. It was observed that at $D_b/D_e = 0.8$, the maximum variations in maximum horizontal wall movement were 24.26 and 39.1% for Profiles 1 and 2, respectively.

Figs. 8(a and b) show that the minimum vertical ground displacements were obtained for System 3A, where the first-, second-, third-, and fourth-level struts were 0.10, 0.35, 0.60, and 0.85 times the excavation depth, respectively, for both soil profiles. At $D_b/D_e = 0.8$, the maximum variations in maximum horizontal wall movement were 74.5% and 60.6% for Profiles 1 and 2, respectively. Thus, of all the possible four-level strut arrangements, it is observed that Systems 3A and 4A were the most suitable options for an optimum range of design factors for all cases. Thus, for a four-level strut arrangement, if the struts are kept in the range of 0.10–0.15, 0.35, 0.55–0.60, and 0.80–0.85 times the excavation depth for first-, second-, third-, and fourth-level struts, respectively, then the optimum range of design factors can be achieved.

The effects of strut position in the case of excavation depths of 10 m and 15 m are presented in Table 6. It can be seen that when, $D_e = 10$ m, for a particular value of $D_b/D_e = 1.0$, the forces in the first- and second-level struts were lowest in Systems 1B and 5B, respectively, for both soil profiles. When, $D_e = 15$ m, for a particular value of $D_b/D_e = 1.0$, the forces in the first-, second-, and third-level struts were lowest in Systems 1C (or 2C), 1C, and 5C, respectively, for both soil profiles. The maximum variations in force at the first and second struts for two-level strut systems were 38.25 and 69.3 and 34. % and 75.1% for Soil Profiles 1 and 2, respectively. Similarly, the maximum variations in force at the first, second, and third struts for three-level strut systems were 37.1, 32.6, and 73.9%, and 27.4, 32.8, and 73.1% for Soil Profiles 1 and 2, respectively. When $D_e = 10$ m, the value of the maximum wall moment was minimum in System 4B for both soil profiles. The maximum variations in maximum wall moment under different strut arrangements were 39.2 and 20.0% for Profiles 1 and 2, respectively. When $D_e = 15$ m, the minimum value of maximum wall moment was obtained in System 4C for both soil profiles. The maximum variations in maximum wall moment were 19.3 and 19.5% for Profiles 1 and 2, respectively. When $D_e = 10$ m,

Int. J. Geomech. 2013.13:234-247.

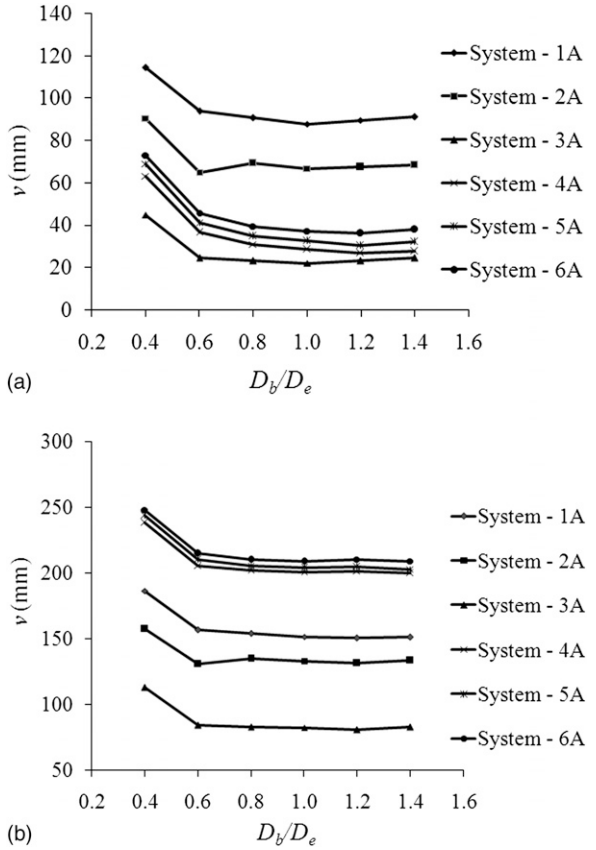

Fig. 8. Variation in ν with D_b/D_e: (a) Soil Profile 1; (b) Soil Profile 2

the value of the maximum lateral wall displacement was minimum in System 1B for both soil profiles. The maximum variations in maximum lateral wall displacement were 29.8 and 65.7% for Profiles 1 and 2, respectively. For $D_e = 15$ m, the minimum value for the maximum lateral wall displacement was obtained in System 4C for both soil profiles. The maximum variations in maximum lateral wall displacement were 9.7 and 54.9% for Profiles 1 and 2, respectively. The minimum value of maximum ground displacement for both soil profiles was obtained in System 1B for the two-level strut system, whereas, for the three-level strut system, the minimum value of maximum ground displacement was obtained in System 1C or 2C. In the two-level strut system, the maximum variations in maximum ground displacement under different strut arrangements were 79.4 and 74.1% for soil Profiles 1 and 2, respectively. In the three-level strut system, the variations were 72.8 and 71.8%, respectively.

Table 6 shows that the lowest range of values of horizontal wall displacements (u) and vertical displacements (v) were obtained for Systems 1B and 2B, where the first and second struts were 0.2 and 0.6–0.7 times the excavation depth. When the excavation depth was 15 m, a similar result was obtained for Systems 1C and 2C, where the first-, second-, and third-level struts were 0.13, 0.4, and 0.67–0.73 times the excavation depth, respectively, for both soil profiles. The bending moment and strut forces were also in the lower range with these strut arrangements. Thus, for $D_e \leq 10$ m, if the first- and second-level struts are placed at 20 and 60–70% of excavation depth, then the lower range of the value of maximum lateral wall displacement and maximum ground displacement can be achieved. Similar conditions can be achieved for $D_e \leq 15$ m, when the first-, second-, and third-level struts are placed at 10–15, 40, and 65–75% of the excavation depth, respectively.

Table 6. Variations in F, M, u, and ν for Systems 1B to 5B and Systems 1C to 5C for Profiles 1 and 2

System number	Strut number	Depth of strut/D_e	$F \times 10^3$ (kN/m)		$M \times 10^3$ (kN·m/m)		u (mm)		ν(mm)	
			Profile 1	Profile 2	Profile 1	Profile 2	Profile 1	Profile 2	Profile 1	Profile 2
1B	1	0.20	2.97	4.16	0.69	1.31	53.0	89.2	4.6	56.5
	2	0.60	6.18	6.53						
2B	1	0.20	3.71	5.04	0.93	1.60	57.5	98.6	4.7	60.0
	2	0.70	4.09	3.91						
3B	1	0.30	3.03	4.06	0.63	1.28	75.5	260.2	18.9	209.2
	2	0.60	7.16	8.35						
4B	1	0.30	3.93	5.15	0.59	1.28	75.4	260.2	20.0	211.9
	2	0.70	4.52	4.86						
5B	1	0.30	4.81	6.17	0.97	1.58	75.5	260.2	22.3	217.7
	2	0.80	2.20	2.08						
1C	1	0.13	2.92	3.92	1.40	1.52	83.1	104.7	7.3	55.4
	2	0.40	8.40	8.66						
	3	0.67	11.10	10.70						
2C	1	0.13	2.92	3.92	1.35	1.49	83.3	105.9	7.1	56.2
	2	0.40	10.85	11.12						
	3	0.73	8.30	7.77						
3C	1	0.13	3.59	4.70	1.37	1.74	86.3	113.4	7.3	61.2
	2	0.47	11.16	10.81						
	3	0.80	5.68	5.43						
4C	1	0.20	3.79	4.52	1.13	1.40	83.0	232.2	19.0	188.5
	2	0.47	9.54	10.22						
	3	0.73	8.77	8.74						
5C	1	0.20	4.64	5.40	1.38	1.40	91.9	232.2	26.1	196.3
	2	0.53	12.46	12.80						
	3	0.87	2.90	2.88						

Int. J. Geomech. 2013.13:234-247.

Effect of Stiffness of Strut

Four different strut stiffnesses (k_{strut}) (1×10^5, 5×10^5, 25×10^5, and 125×10^5 kN/m/m) were considered to study the effect of strut stiffness on design factors, which was studied for a particular arrangement of struts (i.e., for Systems 3A, 1B, and 2C). In the current analysis, the same stiffness was considered for all struts. Each value of strut stiffness was studied for D_b/D_e equal to 0.6, 1.0, and 1.4. Figs. 9 (a and b)–12 show the effect of strut stiffness (k_{strut}) on maximum strut force, maximum wall moment, maximum lateral wall displacement, and maximum vertical ground displacement for both soil profiles. It was observed that for a particular value of D_b/D_e, with the increment of strut stiffness, the strut force also increased up to a stiffness value of 25×10^5 kN/m/m, after which it became constant. Figs. 9(a and b) show that when $D_e = 20$ m and $D_b/D_e = 1.0$, the maximum variations in force (between the highest and lowest values) for first-, second-, third-, and fourth-level struts were 10.9, 21.3, 28.2, and 30.4% for Soil Profile 1 and 5.5, 18.6, 27.8, and 29.5% for Soil Profile 2. In addition, it can be seen that when k_{strut} varied from 5×10^5 to 25×10^5 kN/m/m, the variations in strut forces were 2.9, 5.0, 8.5, and 9.5% for Profile 1 and 0.8, 3.9, 7.8, and 8.8% for Profile 2. The maximum variations in strut force when $D_e = 10$ and 15 m were obtained from numerical analysis and are presented in Table 7. When the depth of excavation was 10 m, the maximum variations in strut force for first- and second-level struts were 12.7 and 30.5% for Profile 1 and 5.1 and 26.2% for Profile 2. However, when the strut stiffness varied from 5×10^5 to 25×10^5 kN/m/m, the variations in strut force were 2.9 and 8.8% for Profile 1 and 1.9 and 6.2% for Profile 2. Similarly, when the depth of excavation was 15 m, the maximum variations in force in first-, second-, and third-level struts were 13.9, 27.4, and 44.6% for Profile 1 and 5.6, 24.5, and 30.0% for Profile 2. However, when the strut stiffness varied from 5×10^5 to 25×10^5 kN/m/m, the variations in strut forces were 4.9, 6.6, and 10.0% for Profile 1 and 1.3, 4.9, and 9.3% for Profile 2.

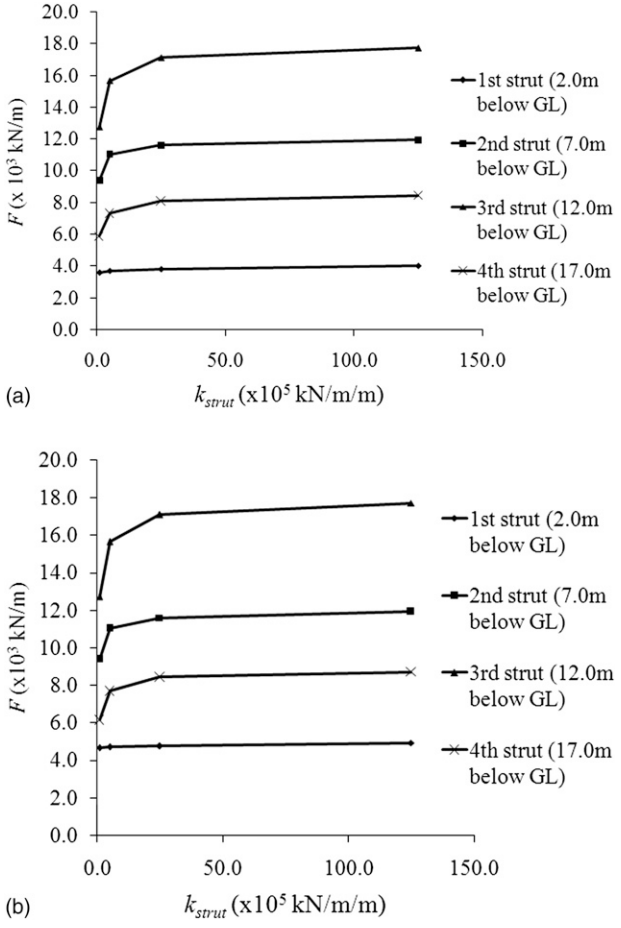

Fig. 9. Variation in F with k_{strut} for $D_b/D_e = 1.0$ and $D_b = 20.0$ m: (a) Soil Profile 1; (b) Soil Profile 2

For a particular value of D_b/D_e, with the increment of strut stiffness, the maximum moment decreased up to a stiffness value of 25×10^5 kN/m/m, after which it became constant for both soil profiles. In Fig. 10, it can be seen that the when $D_e = 20$ m and $D_b/D_e = 1.0$, the maximum variations in wall moment (M) were 18.3% for both soil profiles. It is also seen that when k_{strut} varied from 5×10^5 to 25×10^5 kN/m/m, the variations in the values of M were only 4.5 and 5.1% for Profiles 1 and 2, respectively. For $D_b/D_e = 1.0$, the maximum variations in M (when $D_e = 10$ and 15 m) obtained from numerical analysis are presented in Table 7. When the depth of excavation was 10 m, the maximum variations in moment were 25.6 and 16.1% for Profile 1 and Profile 2, respectively. However, when the strut stiffness varied from 5×10^5 to 25×10^5 kN/m/m, the variations in M were 7.2 and 4.6% for Profiles 1 and 2, respectively. Similarly, it was found that when $D_e = 15$ m,

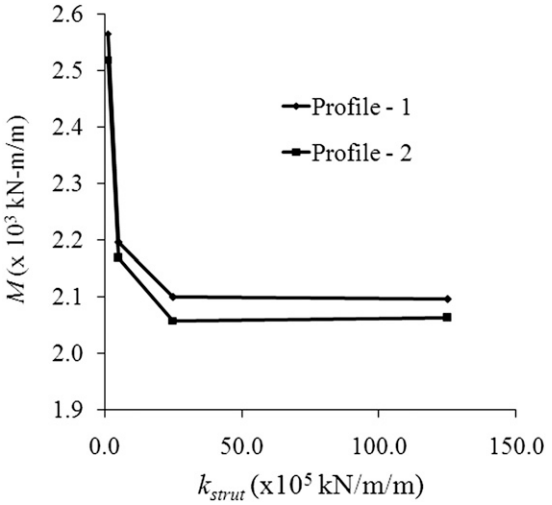

Fig. 10. Variation in M with K_{strut} for $D_b/D_e = 1.0$ and $D_b = 20.0$ m

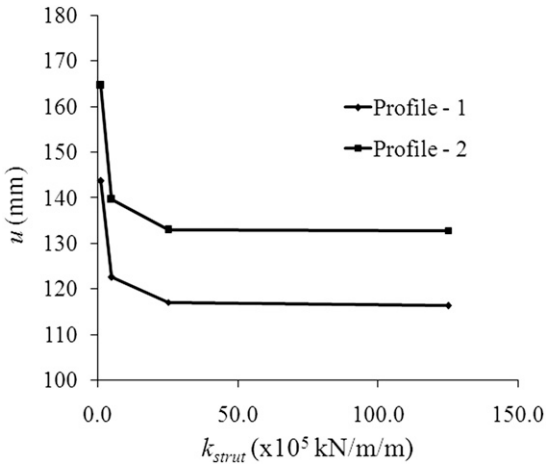

Fig. 11. Variation in u with k_{strut} for $D_b/D_e = 1.0$ and $D_b = 20.0$ m

the maximum variations in moment were 21.5 and 21.6% for Profiles 1 and 2, respectively. However, when the strut stiffness varied from 5×10^5 to 25×10^5 kN/m/m, the variations in values of maximum wall moment were only 5.2 and 4.7% for Profiles 1 and 2, respectively.

For a particular value of D_b/D_e, with the increment of strut stiffness, the maximum wall displacement decreased up to a stiffness value of 25×10^5 kN/m/m, after which it became constant. In Fig. 11, it can be seen that the when $D_e = 20$ m and $D_b/D_e = 1.0$, the maximum variations in wall displacement (u) were 19 and 19.3% for Soil Profiles 1 and 2, respectively. It can also be seen that when k_{strut} varies from 5×10^5 to 25×10^5 kN/m/m, the variations in the values of maximum lateral wall displacement were only 4.6 and 4.7% for Profiles 1 and 2, respectively. For $D_b/D_e = 1.0$, the maximum variation in maximum lateral wall displacement when

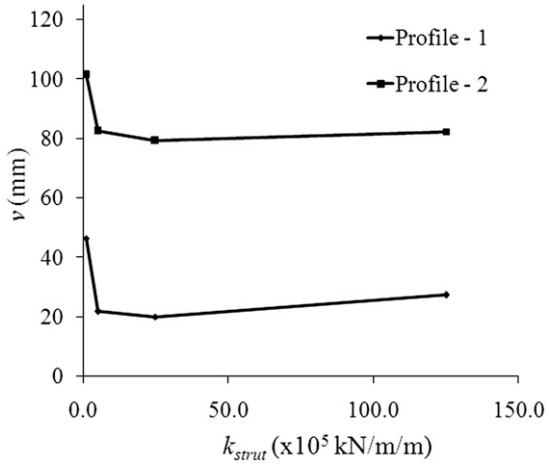

Fig. 12. Variation in ν with k_{strut} for $D_b/D_e = 1.0$ and $D_e = 20.0$ m

$D_e = 10$ m and 15 m are shown in Table 7. When the depth of excavation was 10 m, the maximum variations in maximum lateral wall displacement were 10.9 and 10.2% for Profiles 1 and 2, respectively. When the strut stiffness varied from 5×10^5 to 25×10^5 kN/m/m, these values of maximum lateral wall displacement were only 2.8 and 0.6% for Profiles 1 and 2, respectively. When $D_e = 15$ m, the maximum variations in maximum lateral wall displacement were 16.7 and 17.5% for Profiles 1 and 2, respectively. However, when the strut stiffness varied from 5×10^5 to 25×10^5 kN/m/m, the variations in maximum lateral wall displacement were only 4.3 and 1.1% for Profiles 1 and 2, respectively.

Similar to previous observations for a particular value of D_b/D_e, with the increment of strut stiffness the vertical ground displacement decreased up to a stiffness value of 25×10^5 kN/m/m, after which it became constant or increased slightly. This happened because of the increase in the overall stiffness of the wall-strut system as the stiffness of the struts increased. Thus, when other parameters are kept constant, for a particular soil profile there is no substantial change in displacements (either horizontal or vertical) for a higher value of strut stiffness. In Fig. 12, it can be seen that when $D_e = 20$ m and $D_b/D_e = 1.0$, the maximum variations in vertical ground displacement (v) were 56.8 and 21.9% for soil Profiles 1 and 2, respectively. It is also seen that if k_{strut} varied from 5×10^5 to 25×10^5 kN/m/m, the variations in the value of maximum ground surface displacement were only 8.2 and 3.9% for Profiles 1 and 2, respectively. For $D_b/D_e = 1.0$, the maximum variation in maximum ground surface displacement (at $D_e = 10$ and 15 m) was obtained from numerical analysis and is presented in Table 7. When the depth of excavation was 10 m, the maximum variations in maximum ground surface displacement were 10.9 and 18.4% for Profiles 1 and 2, respectively. When the strut stiffness varied from 5×10^5 to 25×10^5 kN/m/m, the variations in maximum ground surface displacement were 8 and 8.6% for Profiles 1 and 2, respectively. Similarly, when $D_e = 15$ m, the maximum variations in maximum

Table 7. Variations in F, M, u, and ν, with k_{strut} for Both Profiles (1 and 2) (for $D_e = 15.0$ m and 10.0 m)

k_{strut} (kN/m/m)	Strut number	$F \times 10^3$ (kN/m)		$M \times 10^3$ (kN·m/m)		u (mm)		ν (mm)	
		Profile 1	Profile 2	Profile 1	Profile 2	Profile 1	Profile 2	Profile 1	Profile 2
For $D_e = 15.0$ m									
1.0×10^5	1	2.84	3.87	1.63	1.80	95.6	122.0	12.1	64.6
	2	8.71	9.07						
	3	6.73	6.32						
5.0×10^5	1	2.92	3.92	1.35	1.49	83.3	105.9	7.1	56.2
	2	10.85	11.12						
	3	8.30	7.77						
2.5×10^6	1	3.07	3.97	1.28	1.42	79.7	101.4	8.0	55.6
	2	11.62	11.69						
	3	9.22	8.57						
1.25×10^7	1	3.30	4.10	1.33	1.41	79.6	100.7	12.8	63.0
	2	11.99	12.02						
	3	9.73	99.03						
For $D_e = 10.0$ m									
1.0×10^5	1	2.88	4.10	0.86	1.49	57.7	96.6	5.0	50.4
	2	4.80	5.21						
5.0×10^5	1	2.97	4.16	0.69	1.31	53.0	89.2	4.6	56.5
	2	6.18	6.53						
2.5×10^6	1	3.06	4.24	0.64	1.25	51.5	89.7	5.0	61.8
	2	6.78	6.96						
1.25×10^7	1	3.30	4.32	0.65	1.25	51.4	86.7	5.1	61.7
	2	6.91	7.06						

Int. J. Geomech. 2013.13:234-247.

ground surface displacement were 44.5 and 16.2% for Profiles 1 and 2, respectively. When the strut stiffness varied from 5×10^5 to 25×10^5 kN/m/m, the variations in maximum ground surface displacement were 11.25 and 1.1% for Profiles 1 and 2, respectively. Thus, it appears that the optimum value of strut stiffness (25×10^5 kN/m/m) could be determined beyond which no further changes in strut force, moment in the wall, lateral deflection of the wall, or vertical displacement of the ground surface were observed. However, changes in the values of the design factors were very marginal as compared with their maximum variation when strut stiffness changed from 5×10^5 to 25×10^5 kN/m/m. Thus, it can be concluded that if the strut stiffness is chosen to be between 5×10^5 and 25×10^5 kN/m/m, an optimum value of the design factors can be achieved. This range is chosen to make the strut force as low as possible because from the study it was found that the value of strut force increases with the increase in strut stiffness, whereas all other design factors decrease as strut stiffness increases.

Effect of Wall Thickness

Five different values of thickness of the diaphragm wall (i.e., 0.8, 1.0, 1.2, 1.4, and 1.6 m) were considered to study its effect on the behavior of the different design factors for System 3A at $D_e = 20$ m and $D_b/D_e = 0.6$, 1.0, and 1.4. The effect of wall thickness (t_{wall}) on maximum strut force (F) is shown in Table 8. The variations in maximum wall moment (M), maximum lateral wall deflection (u), and maximum vertical ground displacement (v) for Soil Profiles 1 and 2 are shown in Figs. 13–15, respectively, for $D_b/D_e = 1.0$. It was observed that for any value of D_b/D_e and for any profile, the forces in the third- and fourth-level struts decreased with an increase in wall thickness, and this behavior was the opposite for first- and second-level struts.

Table 8 shows that for $D_b/D_e = 1.0$, the maximum variations in forces in first-, second-, third-, and fourth-level struts were 28.8, 19.1, 6.4, and 15.1%, respectively, for Profile 1. The maximum variations in forces in first-, second-, third-, and fourth-level struts were 17.5, 17.8, 8, and 16.9%, respectively, for Profile 2.

It can also be seen that for a particular value of D_b/D_e, the value of the maximum wall moment increased with an increase in the nondimensional parameter, t_{wall}/D_e. A similar trend was observed for both soil profiles. In Fig. 13, it can be seen that for $D_b/D_e = 1.0$, the maximum variations in maximum wall moment (M) were 47.5 and 44.1% for Profiles 1 and 2, respectively.

Fig. 14 shows that the maximum lateral wall displacement (u) decreased with increasing wall thickness. It is also seen that the maximum variations in the values of maximum lateral wall displacement were 36.4 and 40.1% for Profiles 1 and 2, respectively. However, the rate of reduction decreased as the thickness of the wall increased. It can be seen from Fig. 15 that maximum ground surface displacement decreased as t_{wall}/D_e increased. The maximum variations in maximum ground surface displacement were 53 and 82.3% for Profiles 1 and 2, respectively. Thus, it can be concluded that the most sensitive design factor is maximum ground surface displacement with respect to the t_{wall}/D_e value.

As the thickness of the wall increased, forces in the third- and fourth-level struts decreased, whereas in first- and second-level struts, forces increased. Maximum bending moment in the wall increased as the thickness of the wall increased, whereas the trend was reversed in the case of maximum lateral wall displacement. Based on these observations, it appears that an optimum value of wall thickness cannot be determined, although in the case of maximum lateral wall displacement, the rate of reduction decreased as the wall thickness increased. However, in the case of vertical displacement, as the wall thickness increased, displacement decreased up to a certain value of t_{wall}/D_e, after which very little change was observed. For Soil Profile 1, the vertical displacement value was constant when t_{wall}/D_e was greater than 0.05, whereas for Soil Profile 2, very little change was observed when t_{wall}/D_e was greater than 0.07. Thus, based on the observation for vertical displacement, it appears that if t_{wall}/D_e is kept at approximately 0.06–0.07, then an overall optimum result can be obtained. This value can be used as a nondimensional design parameter by giving equal preference to all design factors.

The factor of safety was checked considering three types of strut arrangements, 3A, 1B, and 2C, for $t_{wall}/D_e = 0.06$, strut stiffness = 5×10^5 kN/m/m, and two values of D_b/D_e (i.e., 1.0 and 0.8). The values of the parameters for factor of safety calculations were selected based on the design guidance as reported in this paper. The minimum and maximum values of factor of safety from all the studies were 3.85 and 4.88, respectively. These values are greater than the normally adopted factor of safety value of 2.0 (Bose and Som 1998).

Table 8. Variation in F with t_{wall}/D_e for $D_e = 20.0$ m and Both Profiles (1 and 2)

	$F \times 10^3$ (kN/m)									
	t_{wall}/D_e for Soil Profile 1					t_{wall}/D_e for Soil Profile 2				
D_b/D_e	0.04	0.05	0.06	0.07	0.08	0.04	0.05	0.06	0.07	0.08
0.6	3.6	3.9	4.3	4.7	5.1	4.7	4.8	5.1	5.4	5.8
	11.1	11.9	12.6	13.3	13.9	10.7	11.4	12.1	12.8	13.2
	16.3	15.8	15.3	14.9	14.6	17.0	16.3	15.7	15.3	15.0
	7.6	7.3	6.8	6.5	6.4	8.0	7.7	7.3	6.9	6.8
1.0	3.7	4.0	4.4	4.8	5.2	4.7	4.9	5.1	5.4	5.7
	11.0	11.8	12.4	13.0	13.6	10.6	11.2	11.8	12.4	12.9
	15.7	15.3	15.0	14.8	14.7	16.2	15.7	15.3	15.1	14.9
	7.3	7.1	6.8	6.5	6.2	7.7	7.3	7.1	6.7	6.4
1.4	3.8	4.1	4.5	4.9	5.2	4.7	4.9	5.2	5. 5	5.7
	11.1	11.8	12.4	13.0	13.4	10.6	11.2	11.8	12.3	12.7
	15.7	15.3	15.0	14.6	14.6	16.2	15.7	15.2	14.9	14.6
	7.3	7.1	6.7	6.5	6.1	7.5	7.2	6.9	6.6	6.4

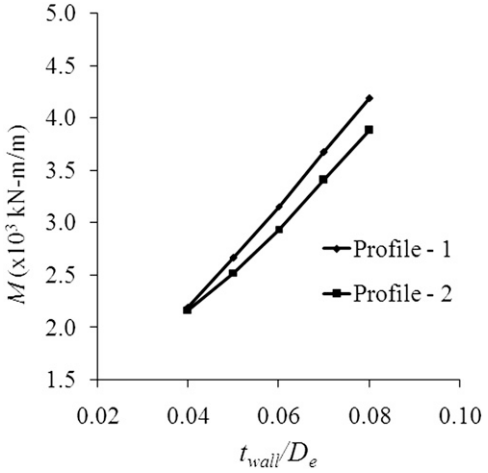

Fig. 13. Variation in M with t_{wall}/D_e for $D_b/D_e = 1.0$ and $D_e = 20.0$ m

Guidance for Design

Based on the results of the current study, the following design guidelines are offered for estimating design parameters.

Int. J. Geomech. 2013.13:234-247.

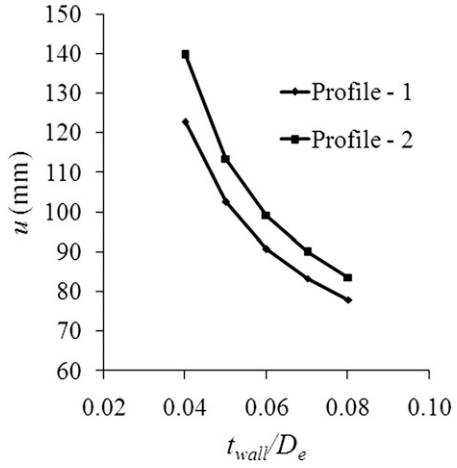

Fig. 14. Variation in u with t_{wall}/D_e for $D_b/D_e = 1.0$ and $D_e = 20.0$ m

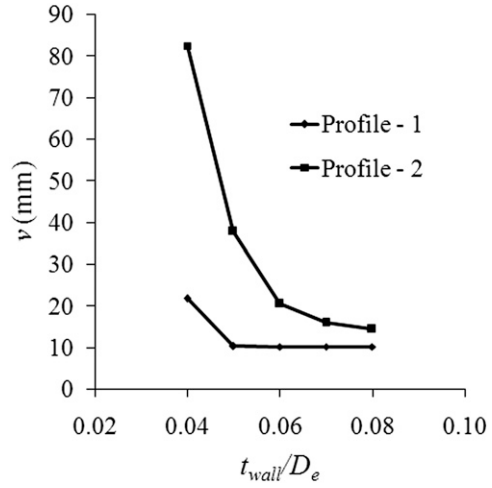

Fig. 15. Variation in ν with t_{wall}/D_e for $D_b/D_e = 1.0$ and $D_e = 20.0$ m

Choose the wall thickness such that t_{wall} is approximately 6–7% of D_e. This thickness is recommended because it gives equal preference to all design factors. However, if there is a preference for a particular design factor, then the thickness has to be chosen according to that preference.

As per the excavation depth, the number of struts in the vertical direction will vary. The required number of struts for different excavation depths is shown in Table 9. The first-level strut should be installed in such a way that the cantilever height of the retaining wall does not produce a high bending moment in the wall or a high deflection of the wall. After the level of the top-most strut is fixed, the number and positions of the other struts should be selected such that a large unsupported length of the wall is prevented, and thus, the axial force in the struts, the wall deflection, and the lateral deflection values are not large. These criteria can be followed for the installation of struts at other levels and for establishing the distance between the excavation base and the lower-most strut level.

The embedded depth of the wall below the final excavation level may be between 0.8 D_e and 1.0 D_e.

The wall stiffness is defined as

$$k_{\text{wall}} = \frac{E_{\text{wall}} I_{\text{wall}}}{h^4} \tag{4}$$

Table 9. Guidance for Numbers and Positions of Struts for Different Excavation Depths

Depth of excavation	Number of struts	Depth of struts below ground level (m)
$D_e \le 10$ m	2	1: 2.0
		2: 6.0–7.0
10 m $< D_e \le 15$ m	3	1: 2.0
		2: 6.0–7.0
		3: 10.0–12.0
15 m $< D_e \le 20$ m	4	1: 2.0
		2: 6.0–7.0
		3: 10.0–12.0
		4: 16.0–17.0

where k_{wall} = stiffness of wall; E_{wall} = modulus of elasticity of wall; I_{wall} = moment of inertia of wall; and h = average vertical spacing of support layers (struts), which is given by

$$h = \frac{\sum h_i}{N} \tag{5}$$

where N = number of support layers. If the first-, second-, third-, and fourth-level struts are at 2 m, 7 m, 12 m, and 17 m below GL and $D_e = 20$ m, the average spacing of struts is calculated as $h = [(7.0 - 2.0) + (12.0 - 7.0) + (17.0 - 12.0) + (20.0 - 17.0)]/4.0 = 4.5$ m. Therefore, for average $t_{\text{wall}} = 1$ m and $E_{\text{wall}} = 2.5 \times 10^7$ kPa, the value of wall stiffness is calculated as $k_{\text{wall}} = 5{,}080.53$ kN/m/m.

The strut stiffness is defined as

$$k_{\text{strut}} = \frac{A_{\text{strut}} E_{\text{strut}}}{ls} \tag{6}$$

where k_{strut} = stiffness of strut; A_{strut} = cross-sectional area of strut; E_{strut} = modulus of elasticity of strut; l = half length of each strut; and s = horizontal spacing of each strut. For $l = 10$ m (i.e., if the excavation is symmetrical with width $B = 20$ m), $s = 10$ m, and $E_{\text{strut}} = 200$ GPa (for steel), A_{strut} is varied to achieve different stiffnesses. Based on the current study, the recommended optimum range of k_{strut} is $(5 \times 10^5 - 25 \times 10^5)$ kN/m/m. Thus, when $D_e = 20$ m, the wall stiffness (k_{wall}) can be kept as 0.20–1.02% of k_{strut} to achieve optimum results.

When the depth of the excavation is 15 m, if the positions of first-, second-, and third-level struts are at 2, 6, and 11 m below GL, respectively, then h is calculated as 4.33 m. The value of k_{wall} is then 5,926.62 kN/m/m. Thus, when $D_e = 15$ m, the wall stiffness (k_{wall}) can be kept as 0.24–1.18% of k_{strut} to achieve optimum results.

When the depth of the excavation is 10 m, if the positions of the first- and second-level struts are at 2 and 6 m below GL, respectively, then h is calculated as 4 m. The value of k_{wall} is then 8,138.02 kN/m/m. In the case of $D_e = 10$ m, the wall stiffness (k_{wall}) can be kept as 0.33–1.63% of k_{strut} to achieve optimum results. Thus, at a particular wall thickness and for a greater excavation depth, a lower range of stiffness of the wall can be used. The calculation of wall stiffness is shown for a particular wall thickness for all three excavation depths. However, if different wall thicknesses are used for different excavation depths (6–7% of depth of excavation as recommended), then the stiffness of the wall has to be calculated by considering the adopted thickness and other chosen quantities. Similarly, the recommended range of wall stiffness can also be determined by correlating with the recommended optimum range of strut stiffness.

Therefore, with all these input parameters, the braced excavation can be analyzed to estimate the maximum strut forces (F), the

Int. J. Geomech. 2013.13:234-247.

maximum bending moment (M) induced in the wall, the maximum horizontal displacement (u) of the wall, and the maximum vertical ground surface displacement (v). The lateral wall displacement (u) depends on the soil type and the wall type, and, above all, on the client's requirements. First, the value of u should be checked, to ensure that it is within permissible limits to satisfy the aforementioned criteria. Similarly, if there are adjacent structures, these should be monitored so that the vertical displacement of the ground (v) does not cause failure of the structures or lead to unacceptable deformation. If these are within the specified limits, then the struts and the wall should be designed for maximum strut force and maximum wall moment, respectively. If the values of maximum lateral wall displacement and maximum vertical ground surface displacement are not within the permissible limits, the strut stiffness and wall stiffness should be adjusted to ensure that these values are within a reasonable limit. Again, the safety of the struts and the wall should be checked against F and M, respectively. If the structural members are safe, then the design is satisfactory from all aspects. The proposed guidelines will help chose design parameters to get the optimum value of important design factors such as strut force, moment in the wall, horizontal deformation of the wall, and vertical ground deformation, because they give equal preference to all factors. However, the designer can choose the value of the design parameters based on the preference given for a particular factor. In such a case, the results presented in this paper will also help in choosing the proper value of the design parameters.

Conclusions

In the current study, an attempt was made to estimate design parameters for braced excavation. Based on the results of the numerical analyses, a design guideline is also recommended. It was observed that, for a particular wall thickness and strut stiffness, different strut arrangements produced different results for maximum strut force, maximum moment, maximum horizontal wall displacement, and maximum vertical ground surface displacement. Based on these results, for a four-level strut system ($15 < D_e \leq 20$ m), if the first-, second-, third-, and fourth-level struts are located at $0.1D_e$, $(0.3–0.35)D_e$, $(0.5–0.6)D_e$, and $(0.8–0.85)D_e$ below GL, respectively, an optimum result can be obtained. Similarly, for a three-level strut system ($10 < D_e \leq 15$ m), to achieve an optimum result, the positions of the first-, second-, and third-level struts should be at $0.13D_e$, $(0.4–0.47)D_e$, and $(0.67–0.80)D_e$ below GL, respectively. For a two-level strut system ($0\text{m} < D_e \leq 10$ m), the first- and second-level struts should be located at $0.2D_e$ and $(0.6–0.7)D_e$ below GL. Parametric studies with different embedded depths revealed that when $D_b/D_e = 0.8 - 1.0$, optimum results can be obtained. It was found that design factors do not vary much when the strut stiffness exceeds a value of 25×10^5 kN/m/m. Third- and fourth-level strut forces decrease with an increase in wall thickness, whereas the opposite is true for first- and second-level struts. The moment in the wall increases with an increase in wall thickness, but the behavior is completely opposite for both horizontal displacement of the wall and vertical displacement of the ground. It was found that when t_w/D_e is approximately 0.07, there is not much change in the vertical ground displacement values.

Notation

The following symbols are used in this paper:

A_{strut} = cross-sectional area of strut;
A_{wall} = cross-sectional area of wall;
B = width of excavation;
c' = effective cohesion;
D_b = embedded depth (final stage)
D_e = maximum excavation depth (final stage)
E = Young's modulus of soil;
E_{strut} = Young's modulus of strut;
E_{wall} = Young's modulus of wall;
F = maximum axial force in strut;
G = shear modulus of soil;
h_i = vertical spacing of supports (struts)
I_{strut} = moment of inertia of strut;
I_{wall} = moment of inertia of wall;
K = bulk modulus of soil;
K_n = interface normal stiffness between wall and soil;
K_o = coefficient of lateral earth pressure at rest;
K_s = interface shear stiffness between wall and soil;
k_{strut} = strut stiffness;
k_{wall} = wall stiffness;
l = length of strut;
M = maximum bending moment in wall;
N = number of support layers;
s = horizontal spacing of struts;
t_{wall} = thickness of wall;
u = maximum horizontal wall displacement;
v = maximum vertical ground displacement;
γ' = effective unit weight of soil;
$\Delta z_{\min}$ = smallest width of adjoining zone in normal direction to interface;
μ = Poisson's ratio of soil;
μ_{wall} = Poisson's ratio of wall;
ϕ' = effective angle of internal friction; and
ψ = dilation angle of soil.

References

Babu, G. L. S., Srivastava, A., Rao, K. S. N., and Venkatesha, S. (2011). "Analysis and design of vibration isolation system using open trenches." *Int. J. Geomech.*, 11(5), 364–369.

Boscardin, M. D., and Cording, E. J. (1989). "Building response to excavation induced settlement." *J. Geotech. Engrg. Div.*, 115(1), 1–21.

Bose, S. K., and Som, N. N. (1998). "Parametric study of a braced cut by finite element method." *Comput. Geotech.*, 22(2), 91–107.

Bowles, J. E. (1988). *Foundation analysis and design*, 4th Ed., McGraw Hill, New York.

Chungsik, Y., and Dongyeob, L. (2008). "Deep excavation-induced ground surface movement characteristics—A numerical investigation." *Comput. Geotech.*, 35(2), 231–252.

Costa, P. A., Borges, J. L., and Fernandes, M. M. (2007). "Analysis of a braced excavation in soft soils considering the consolidation effect." *J. Geotech. Geol. Eng.*, 25(6) 617–629.

de Lyra Nogueira, C., de Azevedo, R., and Zornberg, J. (2009). "Coupled analyses of excavations in saturated soil." *Int. J. Geomech.*, 9(2), 73–81.

Finno, R. J., Atmatzidis, D. K., and Roboski, J. F. (2007). "Three-dimensional effects for supported excavations in clay." *J. Geotech. Geoenviron. Eng.*, 133(1), 30–36.

Finno, R. J., and Harahap, I. S. (1991). "Finite element analysis of HDR-4 excavation." *J. Geotech. Engrg. Div.*, 117(10), 1590–1609.

Hashash, Y. M. A., and Whittle, A. J. (2002). "Mechanisms of load transfer and arching for braced excavations in clay." *J. Geotech. Geoenviron. Eng.*, 128(3), 187–197.

Int. J. Geomech. 2013.13:234-247.

Hsi, J. P., and Small, J. C. (1993). "Application of a fully coupled method to the analysis of an excavation." *Soils Found.*, 33(4), 36–48.
Hsieh, P. G., and Ou, C. Y. (1998). "Shape of ground surface settlement profiles caused by excavation." *Can. Geotech. J.*, 35(6), 1004–1017.
Hsiung, B. C. B. (2009). "A case study of behavior of deep excavation in sand." *Comput. Geotech.*, 36(4), 665–675.
Itasca. (2005) *User's guide for FLAC version 5.0*., Itasca India Consulting, Nagpur, India.
Karlsrud, K., and Andresen, L. (2005). "Loads on braced excavations in soft clay." *Int. J. Geomech.*, 5(2), 107–113.
Kung, G. T. C. (2009). "Comparison of excavation-induced wall deflection using top-down and bottom-up construction methods in Taipei silty clay." *Comput. Geotech.*, 36(3), 373–385.
Kung, G. T. C., Ou, C. Y., and Juang, C. H. (2009). "Modelling small strain behavior of Taipei clays for finite element analyses of braced excavations." *Comput. Geotech.*, 36(1–2), 304–319.
Nakai, T., Hiromichi, K., Murata, K., Banno, M., and Tadashi, H. (1999). "Model tests and numerical simulation of braced excavation in sandy ground: Influences of construction history, wall friction, wall stiffness, strut position and strut stiffness." *Soils Found.*, 39(3), 1–12.
Ng, C. W. W., and Lings, M. L. (1995). "Effects of modeling soil nonlinearity and wall installation on back-analysis of deep excavation in stiff clay." *J. Geotech. Geoenviron. Eng.*, 121(10), 687–695.
Ng, C. W. W., Simpson, B., Lings, M. L., and Nash, D. F. T. (1998). "Numerical analysis of a multipropped retaining wall in stiff clay." *Can. Geotech. J.*, 35(1), 115–130.
Nogueira, C., Azevedo, R., and Zornberg, J. (2011). "Validation of coupled simulation of excavations in saturated clay: Camboinhas case history." *Int. J. Geomech.*, 11(3), 202–210.
Ou, C. Y., Hsieh, P. G., and Chiou, D. C. (1993). "Characteristics of ground surface settlement during excavation." *Can. Geotech. J.*, 30(5), 758–767.
Seok, J. W., Kim, O. Y., Chung, C. K., and Kim, M. M. (2001). "Evaluation of ground and building settlement near braced excavation sites by model testing." *Can. Geotech. J.*, 38(5), 1127–1133.
Som, N. N., and Das, S. C. (2006). *Theory and practice of foundation design*, Prentice Hall of India Pvt. Ltd., New Delhi, India.
Tefera, T. H., Nordal, S., Grande, L., Sandven, R., and Emdal, A. (2006). "Ground settlement and wall deformation from a large scale model test on a single strutted sheet pile wall in sand." *Int. J. Phys. Numer. Model. Geotech.*, 6(2),1–13.
Vaziri, H. H. (1996). "Numerical study of parameters influencing the response of flexible retaining walls." *Can. Geotech. J.*, 33, 290–308.
Whittle, A. J., Hashash, Y. M. A., and Whitman, R. V. (1993). "Analysis of deep excavation in Boston." *J. Geotech. Engrg.*, 119(1), 69–90.
Zdravkovic, L., Potts, D. M., and St. John, H. D. (2005). "Modeling of a 3D excavation in finite element analysis." *Geotechnique*, 55(7), 497–513.

Int. J. Geomech. 2013.13:234-247.